Supplementary Information

Table S1. Summary of previous applications of CH_3F as a cell gas.

Analyte	Interference	Sample Matrix	Cell Reactions	Reference
$^{87}Sr/^{86}Sr$ ratio	^{87}Rb	Seven materials with different Rb/Sr ratios: 1. Basalt (0.02) 2. Nephelinite (0.03) 3. Basalt (0.11) 4. Basalt (0.55) 5. Basalt (0.14) 6. Diorite (0.28) 7. Rhyolite (0.67)	$^{86,87,88}Sr^+ + CH_3F \rightarrow {}^{86,87,88}SrF^+ + CH_3$	1
^{89}Sr	^{87}Rb	Dissolute magmatic rocks	$M^+ + CH_3F \rightarrow MF^+ + CH_3$	2
^{75}As, $^{77,78,79}Se$	^{75}Se, ^{75}Ge, ^{75}Rb, ^{77}Br, ^{77}Mo, ^{77}Ag, ^{78}Kr, ^{78}Mo, ^{78}Rb, ^{78}Ag, ^{79}Br, ^{79}Kr, ^{79}Rb, ^{79}Mo	Synthetic matrices containing elements giving rise to ions interfering either at the original *m/z* ratios or those of the reaction products	$^{75}As^+ + CH_3F \rightarrow {}^{75}AsCH_2^+ + HF$ $^{77,78,79}Se + CH_3F \rightarrow {}^{77,78,79}SeCH_2^+ + HF$	3
^{75}As and $^{77,78}Se$	$^{40}Ar^{35}Cl^+$, $^{59}Co^{16}O^+$, $^{36}Ar^{38}ArH^+$, $^{38}Ar^{37}Cl^+$, $^{36}Ar^{39}K^+$, $^{43}Ca^{16}O_2^+$, $^{40}Ar^{23}Na^{12}C^+$, $^{12}C^{31}P^{16}O_2^+$, $^{40}Ca^{35}Cl^+$, $^{38}Ar^{37}Cl^+$, $^{40}Ca^{37}Cl^+$, $^{36}Ar^{40}ArH^+$, $^{38}Ar_2H^+$, $^{12}C^{19}F^{14}N^{16}O_2^+$, $^{78}K^+$, $^{40}Ar^{40}Ca^+$, $^{64}Ni^{16}O^+$, $^{64}Zn^{16}O^+$, $^{32}S_2{}^{16}O^+$, $^{32}S^{16}O_3^+$, $^{40}Ar^{40}Ar^+$, and $^{40}Ca^{40}Ca^+$	Certified reference materials (pine needles, tomato leaves, rice flour, tuna fish tissue, fish protein, plankton, estuarine sediment, oyster tissue, lobster hepatopancreas, and Seronorm™)	$M^+ + CH_3F \rightarrow MCH_2^+ + HF$ $M^+ + CH_3F \rightarrow MF^+ + CH_3$ $M^+ + CH_3F \rightarrow MCHF^+ + H_2$ $MF^+ + CH_3F \rightarrow MF_2^+ + CH_3$ $MCH_2^+ + CH_3F \rightarrow MCH_2^+(CH_3F)$	4
La, Ce, Pr, Nd, Sm, Eu, Gd, Tb, Dy, Ho, Er, Tm, Yb, Lu	Lanthanide tailing and hydrides	Vaporised solution containing lanthanide salt	$Ln^+ + CH_3F \rightarrow LnF^+ + CH_3$ $Ln^+ + CH_3F \rightarrow Ln^+(CH_3F)$ (only for Ln = Dy, Ho, Er, Tm, Yb, Lu)	5
Al, Co, Cr, Mn, Ni, Ti, V	C, Ca, Cl, Fe, K, Mg, Na, P, and S	Blood serum and urine	$M^+ + CH_3F \rightarrow MF_a(CH_3F)_b^+$	6

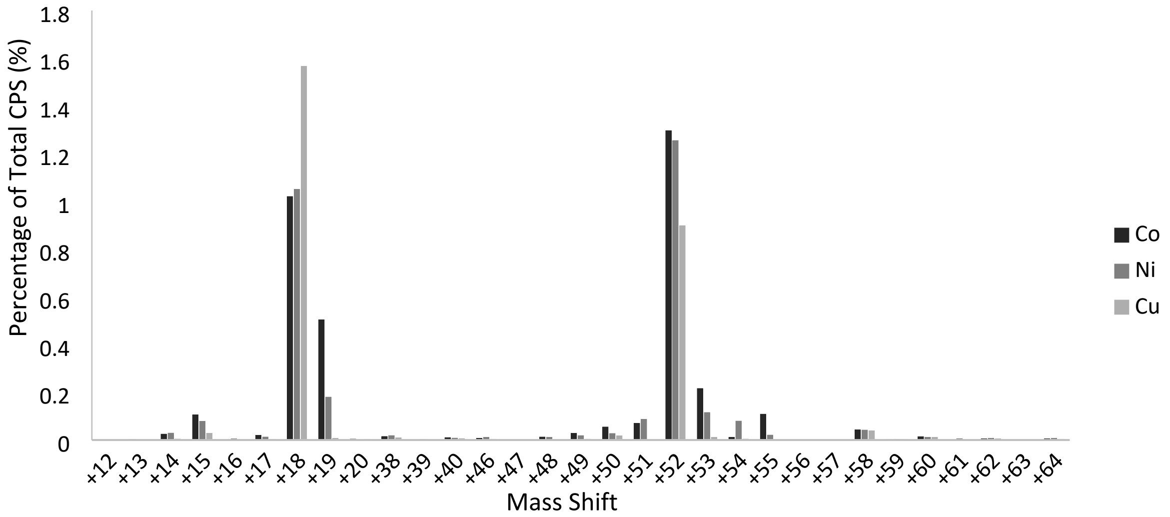

Figure S1. Product ion scan for Co, Ni and Cu using CH_3F with mass shifts from +12 to +64.

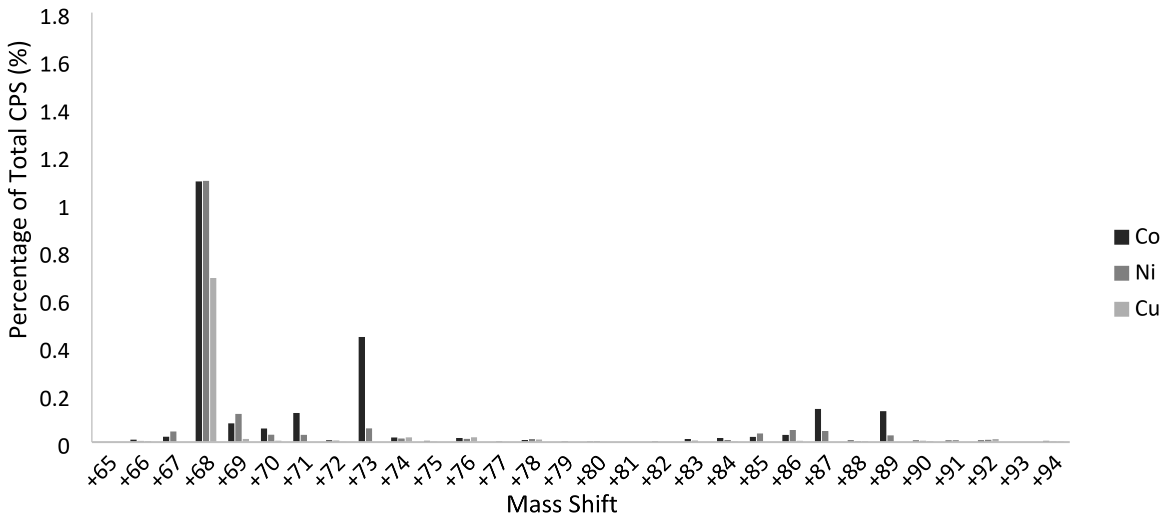

Figure S2. Product ion scan for Co, Ni and Cu using CH_3F with mass shifts from +65 to +94.

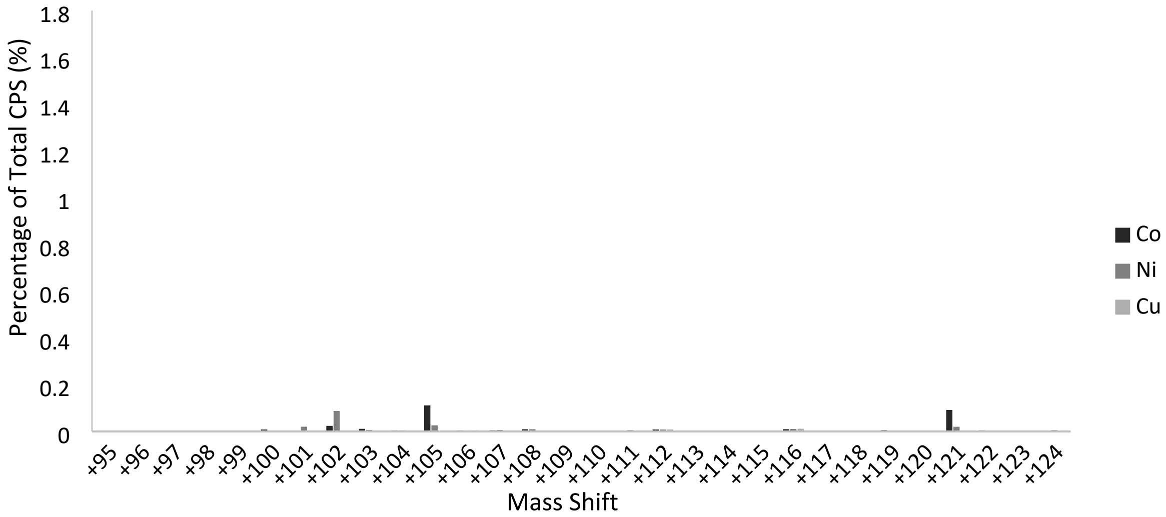

Figure S3. Product ion scan for Co, Ni and Cu using CH_3F with mass shifts from +95 to +124.

Table S2. Summary of the mass shifts measured for each actinide tested.

Actinide	**Mass Shifts**
^{232}Th	On Mass, +19, +34, and +38
^{237}Np	On Mass, +1 to +38
^{238}U	On Mass, +19, and +34
^{239}Pu	On Mass, +1 to +36
^{241}Am	On Mass, +1 to +34

Table S3. Possible separation schemes for actinides, including their optimal CH_3F gas flow rate, cell reaction(s) and mass shift.

Separation Scheme	**CH_3F Gas Flow Rate (mL/min)**	**Mass Shift**	**Cell Reaction**
^{237}Np / ^{239}Pu + ^{241}Am	5	+16	$M^+ + CH_3F \rightarrow MCH_2^+ + HF$ $MCH_2^+ + CH_3F \rightarrow MCH_3 + CH_2F^+$ $MCH_3 + CH_3F \rightarrow MCH_4^+ + CH_2F^-$
^{237}Np / ^{239}Pu + ^{241}Am	2	+19	$M^+ + CH_3F \rightarrow MF^+ + CH_3$
^{232}Th / ^{237}Np	6	+38	$M^+ + CH_3F \rightarrow MF^+ + CH_3$ $MF^+ + CH_3F \rightarrow MF_2^+ + CH_3$

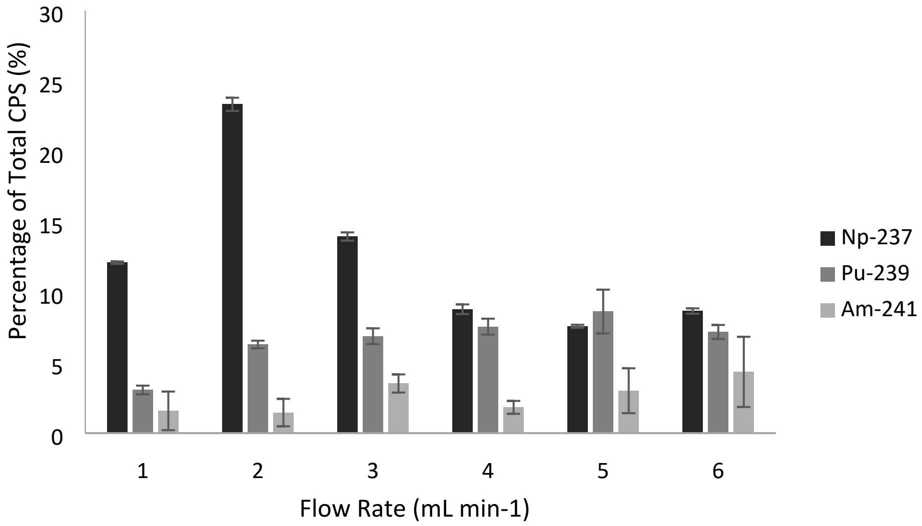

Figure S4. Graph showing the percentage of the total signal for ^{237}Np, ^{239}Pu, and ^{241}Am at mass shift +19 as CH_3F gas flow rate increases.

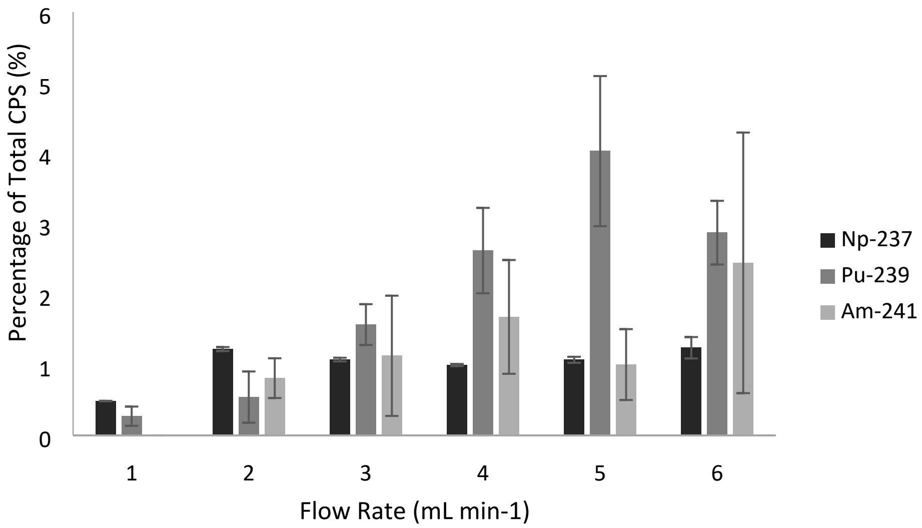

Figure S5. Graph showing the percentage of the total signal for ^{237}Np, ^{239}Pu, and ^{241}Am at mass shift +16 as CH_3F gas flow rate increases.

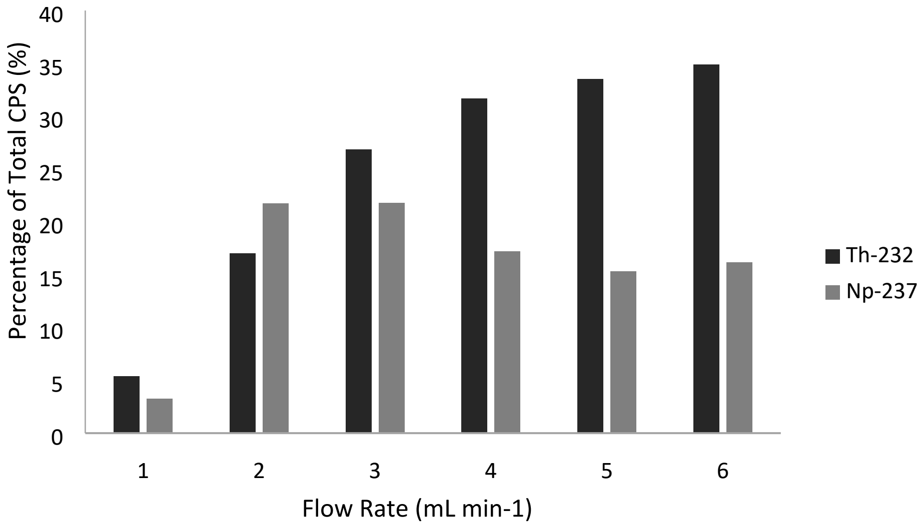

Figure S6. Graph showing the percentage of the total signal for ^{232}Th and ^{237}Np at mass shift +38 as CH_3F gas flow rate increases.

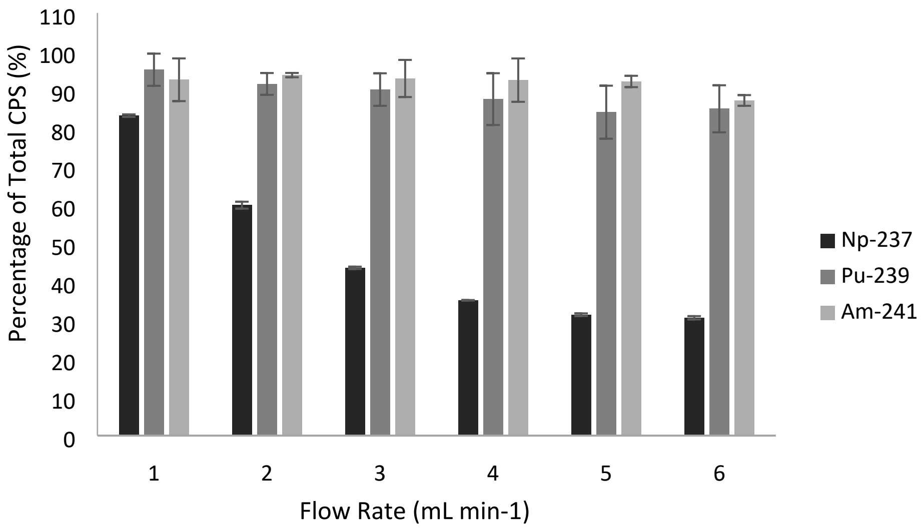

Figure S7. Graph showing the percentage of the total signal for ^{237}Np, ^{239}Pu, and ^{241}Am remaining on mass as CH_3F gas flow rate increases.

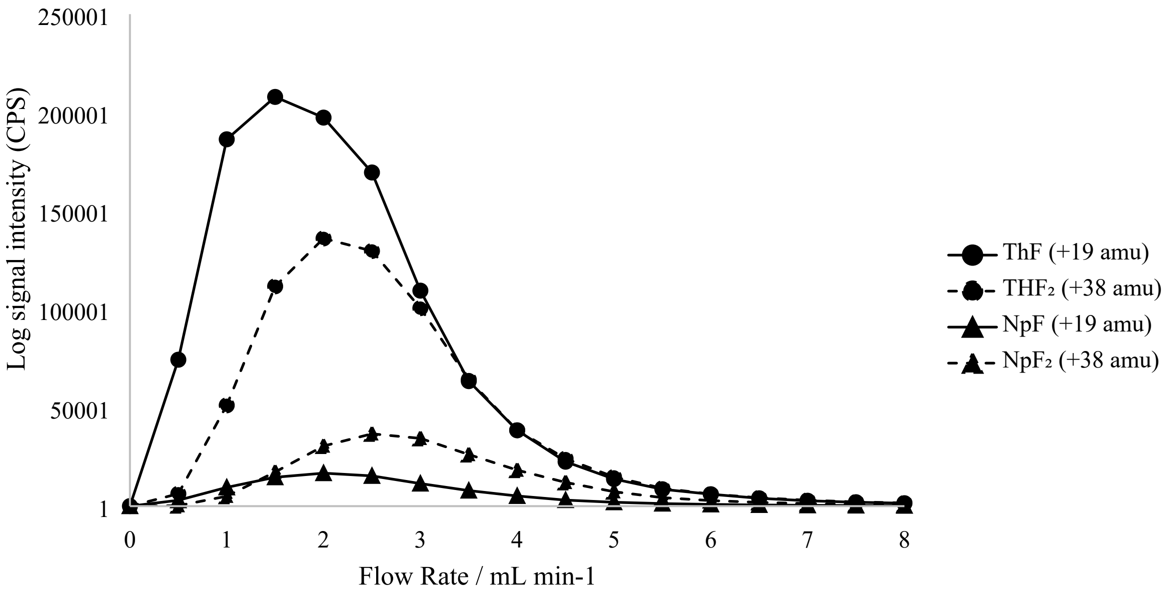

Figure S8. Variation of sensitivity for the formation of the MF (+19 amu) and MF_2 (+38 amu) product ions for ^{232}Th and ^{237}Np with flow rate of CH_3F cell gas.

References

1. E. Bolea-Fernandez, S.J.M. Van Malderen, L. Balcaen, F. Vanhaecke and M. Resano, in *Handbook Of ICP-QQQ Applications Using The Agilent 8800 And 8900*, Agilent Technologies, USA, 5th Edition, 2022, Direct Strontium Isotopic Analysis Of Solid Samples By LA-ICP-MS/MS, 378-381.
2. L.J. Moens, F.F. Vanhaecke, D.R. Bandura, V.I. Baranov and S.D. Tanner, Elimination Of Isobaric Interferences In ICP-MS, Using Ion-Molecule Reaction Chemistry: Rb/Sr Age Determination Of Magmatic Rocks, A Case Study, *J. Anal. At. Spectrom.*, 2001, **16**, 991-994.
3. E. Bolea-Fernandez, L. Balcaen, M. Resanon and F. Vanhaecke, Interference-Free Determination Of Ultra-Trace Concentrations Of Arsenic And Selenium Using Methyl Fluoride As A Reaction Gas In ICP-MS/MS, *Anal. Bioanal. Chem.*, 2015, **407**, 919-929.
4. X. Zhao, G.K. Koyanagi and D.K. Bohme, Reactions Of Methyl Fluoride With Atomic Transition-Metal And Main-Group Cations: Gas-Phase Room-Temperature Kinetics And Periodicities In Reactivity, *J. Phys. Chem. A*, 2006, **110**, 10607-10618.
5. G.K. Koyanagi, X. Zhao, V. Blagojevic, M.J.Y. Jarvis and D.K. Bohme, Gas-Phase Reactions Of Atomic Lanthanide Cations With Methyl Fluoride, *Int. J. Mass. Spectrom.*, 2005, **241**, 189-196.
6. E. Bolea-Fernandez, L. Balcaen, M. Resano and F. Vanhaecke, Potential Of Methyl Fluoride As A Universal Reaction Gas To Overcome Spectral Interference In The Determination Of Ultratrace Concentrations Of Metals In Biofluids Using Inductively Coupled Plasma-Tandem Mass Spectrometry, *Anal. Chem.*, 2014, **86**, 7969-7977.